Journal of Fluids and Structures (1999) **13**, 865–875
Article No.: jfls.1999.0235, available online at http://www.idealibrary.com on IDEAL®

ROBUST CONTROL OF VORTEX-INDUCED VIBRATION OF A RIGID CYLINDER SUPPORTED BY AN ELASTIC BEAM USING μ-SYNTHESIS

J. TANI, J. QIU AND Y. LIU

Institute of Fluid Science, Tohoku University, Sendai 980-8577, Japan

(Received 1 September 1998 and in revised form 20 January 1999)

For lightweight and flexible structures, it is important to suppress the vibrations induced by interactions between fluid and structures. This paper presents the robust control of the vortex-induced vibration of a rigid circular cylinder supported by an elastic cantilever beam in which the fluid force is considered as an external excitation on the structure. For the problems considered here, the excitation frequency is assumed to be equal to the natural frequency of the structure or the "lock-in" frequency. The natural frequencies of this analytical model are calculated by using the modal analysis method and then modal coordinates are introduced to obtain the state equations of the structural system. A pair of piezoelectric devices fixed under the base plate, on which the elastic beam is clamped, were used as actuators. A robust controller satisfying the nominal performance and robust performance is designed using μ-synthesis theory based on the structured singular value. Simulation and experiment were carried out with the designed controller and the effectiveness of the robust control strategy was verified by both experimental and simulation results.

1. INTRODUCTION

UNSTABLE VIBRATIONS SUCH as vortex-induced vibration, galloping, flutter are induced frequently on structures in contact with fluid flow, such as high buildings, ocean structures, aircraft and fluid machines, due to the interaction between elastic structures and fluid. Especially, when a structure is made to move at high speed, these unstable vibrations may occur easily and become a critical factor for the performance of the structure. Therefore, it is important to suppress the flow-induced vibration with active control technology. In the past decades, though a number of studies have been reported on the vibration characteristics of structures exposed to flow and the flow characteristics around structures, there are few studies concerning the active control of flow-induced vibration (Baz & Rao 1991; Baz & Kim 1993; Indrani & Walter 1996; Jonathan 1998). The main difficulty for control is nonlinearity and irregularity in the flow-induced vibration of structures. Since modeling errors are inevitable in the state-space model of structures, robust control is necessary.

In this paper, a study on the robust control of vortex-induced vibration of a rigid circular cylinder supported by an elastic beam and placed in a uniform air flow is presented. A pair of piezoelectric actuators are used to control the motion of the base plate on which the elastic beam is clamped. The natural frequencies of the test model are calculated by using the transfer matrix method and then modal coordinates are introduced to establish state equations of the structural system. A robust controller is designed to suppress the vortex-induced vibration of the cantilever beam using μ-synthesis theory. Experiments were carried out and the results were compared with the simulation results.

0889–9746/99/100865 + 11 $30.00

2. THEORETICAL ANALYSIS

2.1. Equation of Motion

The analytical model is shown schematically in Figure 1. A rigid cylinder is fixed through an elastic beam on a base plate, which is supported by two piezoelectric elements used as actuators. Since the actuators deform in the longitudinal direction, the angle θ between the beam and x-axis can be actively controlled by applying opposite-phase voltage to the two actuators. The cylinder is placed in a uniform air-flow and is subjected to an alternate lift force in the transverse direction (y direction) due to the vortex shedding around the cylinder. The force of air-flow is directly transmitted to the elastic beam, so that a bending vibration is induced in the beam. The vibration of the beam is suppressed by actively controlling the angle θ.

It is supposed that the beam vibrates with small amplitude in the x–y plane and the force of air-flow acts at the mid-point of the cylinder. For simplicity, the rigid cylinder is regarded as a lumped mass at the mid-point and the effective part of the elastic beam is supposed to be from the clamped end ($x = 0$) to the mid-point of the cylinder ($x = L_b$). From these assumptions the equation of motion of the beam can be expressed in the following form:

$$EI\frac{\partial^4 W(x,t)}{\partial x^4} + cEI\frac{\partial^5 W(x,t)}{\partial x^4 \partial t} + [\rho A + m\delta(x - L_b)]\frac{\partial^2 W(x,t)}{\partial t^2}$$
$$= -[\rho A x + mL_b\delta(x - L_b)]\ddot{\theta}(t) + \tfrac{1}{2}\rho_s U_0^2 D_s L_s C_w(t)\delta(x - L_b), \qquad (1)$$

in which the first term on the right-hand side is the inertial force due to variation of θ and the second term is the force of air-flow.

The boundary conditions are given by

$$W(x,t)|_{x=0} = \left.\frac{\partial W(x,t)}{\partial x}\right|_{x=0} = 0,$$
$$\left.\frac{\partial^2 W(x,t)}{\partial x^2}\right|_{x=L_b} = \left.\frac{\partial^3 W(x,t)}{\partial x^3}\right|_{x=L_b} = 0. \qquad (2)$$

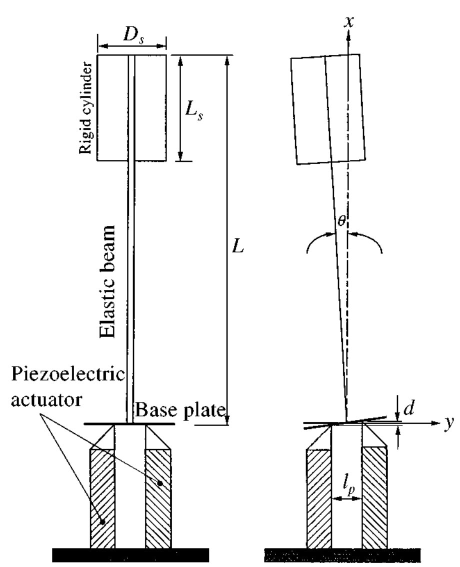

Figure 1. Analytical model and coordinate system.

Considering that the displacement of the piezoelectric actuator is very small, we have

$$\theta(t) = \tan^{-1}[d(t)/l_p] \cong d(t)/l_p. \tag{3}$$

Using the modal expansion method, the solution of equation (1) can be expressed as a summation of modal functions, each multiplied by a function of time as follows:

$$W(x, t) = \sum_{j=1}^{n} \phi_j(x) q_j(t). \tag{4}$$

Substitution of equation (4) into equation (1), multiplication of the result by $\phi_j(x)$ and integration with respect to x from 0 to L_b give a set of ordinary differential equations in modal coordinates:

$$\ddot{q}_j(t) + c\omega_j^2 \dot{q}_j(t) + \omega_j^2 q_j(t) = b_j \ddot{\theta}(t) + f_j C_w(t) \qquad (j = 1, 2 \ldots \infty), \tag{5}$$

where

$$f_j = \frac{\phi(L_b)}{2L_b} \rho_s U_0^2 D_s L_s \tag{6}$$

and

$$b_j = -\frac{1}{L_b}\left[m L_b \phi_j(L_b) + \rho A \int_0^{L_b} x \phi_j(x)\, \mathrm{d}x \right]. \tag{7}$$

2.2. State Equations and Parameters

Neglecting the high-order mode and introducing the state vector

$$\mathbf{x}(t) = [q_1(t), q_2(t), \ldots, q_n(t), \dot{q}_1(t), \dot{q}_2(t), \ldots, \dot{q}_n(t)^{\mathrm{T}}, \tag{8}$$

we can rewrite equation (5) in the following form:

$$\begin{aligned} \dot{\mathbf{x}}(t) &= \mathbf{A}\mathbf{x}(t) + \mathbf{B}u(t) + \mathbf{F}C_w(t), \\ y_c(t) &= \mathbf{C}\mathbf{x}(t), \end{aligned} \tag{9}$$

where $y_c(t)$ is the displacement of the beam at $x = L_b$ which is used as control output, n is the number of considered modes, u is the control input defined as $\ddot{\theta}$, and **A**, **B**, **C**, **F** are defined as follows:

$$\mathbf{A} = \begin{bmatrix} \mathbf{0} & \mathbf{I} \\ \mathbf{diag}(-\omega_j^2) & \mathbf{diag}(-c\omega_j^2) \end{bmatrix}_{2n \times 2n},$$

$$\mathbf{B} = \begin{Bmatrix} 0 \\ \vdots \\ 0 \\ b_1 \\ \vdots \\ b_n \end{Bmatrix}_{2n \times 1}, \qquad \mathbf{F} = \begin{Bmatrix} 0 \\ \vdots \\ 0 \\ f_1 \\ \vdots \\ f_n \end{Bmatrix}_{2n \times 1}, \tag{10}$$

$$\mathbf{C} = [\phi_1(L_b) \cdots \phi_n(L_b) 0 \cdots 0]_{1 \times 2n}.$$

Equation (9) is the state equation of the structural system.

According to the fact that when the vortex-shedding frequency is sufficiently near to the natural frequency of the cylinder resonant transverse vibration occurs and the fluid pressure

TABLE 1
Parameters of test model

Beam		Cylinder	
L	200 mm	L_s	60 mm
H	2·0 mm	D_s	57 mm
B	2·4 mm	m	25·6 g
E	68·6 GPa	l_p	15 mm
ρ	$2{\cdot}7 \times 10^3$ kg/m^3		

acting on the cylinder can be supposed to be a periodical exciting force with the same frequency as the first mode of the elastically supported cylinder (Sumer & Fredsøe 1997). Therefore, $C_w(t)$ can be expressed in the following form:

$$C_w(t) = \bar{C}_w \sin \omega_1 t, \tag{11}$$

where $\bar{C}_w$ is the amplitude of fluid force $C_w(t)$.

The parameters of the physical model are shown in Table 1. From these parameters, the natural frequency of the first mode is estimated to be 7·9 Hz. In this study we consider only the first mode in the state equation, that is, $n = 1$ in equation (8).

3. DESIGN OF CONTROLLER

3.1. μ-SYNTHESIS THEORY

A robust controller was designed for the control system shown in Figure 2 by using the μ-synthesis theory (Balas *et al.* 1991). The block diagram shown in Figure 2 is composed of a nominal model G_{nom}, model error Δ, controller K, weight function W_{del} for uncertainty of the model, and weight function W_p for performance of the controller. The uncertainty of the model is induced by the approximation of the continuous structural systems with a discrete system of finite degrees of freedom, neglect of high-order modes, neglect of the hysteresis of the piezoelectric actuators and other approximations in the modeling process. The nominal model G_{nom} represents the theoretical model expressed by the state equation and Δ is used to parametrize the total error between the real structural systems and nominal model. The model error Δ is unknown, except that it satisfies condition $\|\Delta\|_\infty < 1$.

The closed-loop control system shown in Figure 2 can be transformed to a general plant for μ-synthesis shown in Figure 3, in which M is the transfer function of the sub-system enclosed by the dashed line in Figure 2. Based on Figure 3, we can design a controller K satisfying the robust control performance defined by weight functions W_{del} and W_p. For given weight functions W_{del} and W_p, a μ-synthesis controller is designed based on structured singular value so that the H_∞ norm of M is less than 1.

3.2. DESIGN OF CONTROLLER

In order to design the controller K, weight functions W_{del} and W_p must be determined first. The error of the nominal model is small in the low-frequency range, but it can be significantly large in the high-frequency range since the low-order modes are included in the nominal model but the high-order modes are neglected. On the other hand, high suppression ratio of disturbance is required only in the low-frequency range since only the low-order modes are strongly excited. For the above reason, the following weight functions

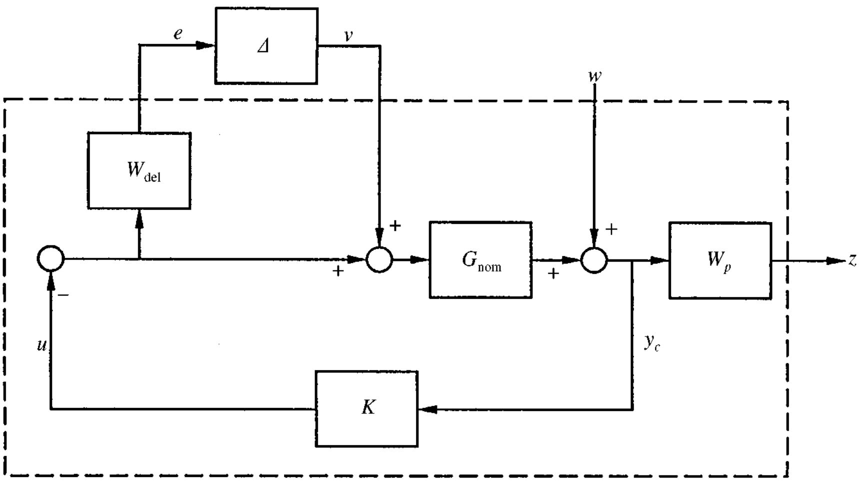

Figure 2. Block diagram of closed-loop system.

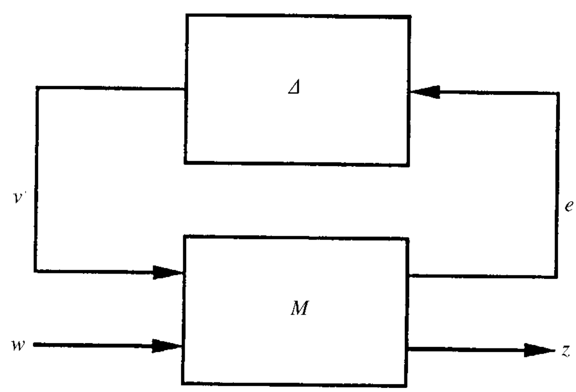

Figure 3. General plant for μ-synthesis.

are chosen and their frequency characteristics are shown in Figure 4:

$$W_{del} = \frac{0{\cdot}3(s+200)}{s+600}, \qquad W_p = \frac{0{\cdot}5(s+400)}{s+40}. \tag{12}$$

The weight function W_{del} means that the modeling error is 10% in the low-frequency range and 30% in the high-frequency range. The function W_p equals 5 in the low-frequency range and 0·5 in the high-frequency range, which means that the disturbance in the output path of the closed-loop system should be reduced by 80% in the low-frequency range and could be amplified by as much as 100% in the high-frequency range.

Using these weight functions and H_∞ control theory, we obtained a controller with which $\gamma = \|M\|_\infty = 1{\cdot}98$. It should be noticed that the robust performance of this system is not satisfied since γ is larger than 1. However, after one step of D–K iteration of the μ-synthesis method, γ is reduced to 0·93, that is, the desired robust performance is satisfied. On the other hand, the order of controller rises to 10 after one-step of D–K iteration. The frequency characteristics of the designed controller is shown in Figure 5. Since the controller is designed on the basis of the continuous-time system and implemented digitally on

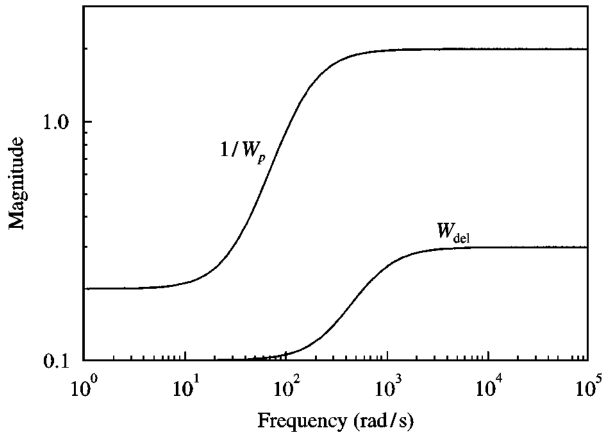

Figure 4. Frequency characteristics of weight functions.

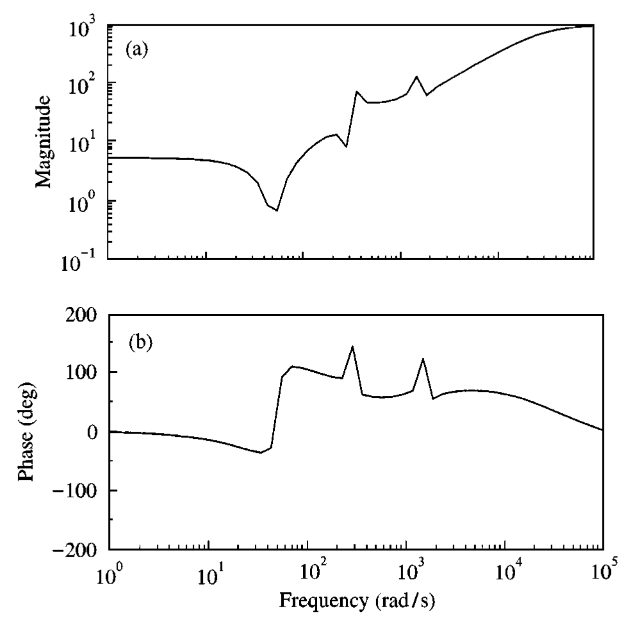

Figure 5. Frequency characteristics of controller: (a) gain; (b) phase.

a personal computer, the sampling frequency should be as high as possible. In order to reduce the amount of computation so as to increase the sampling frequency, the order of controller is reduced from 10 to 6 using an optimal norm approximation. The transfer function of controller after reduction can be expressed in the following form (Glover 1984):

$$K(s) = \frac{571080(s + 26{\cdot}8 - 1560\mathrm{j})}{(s + 89270)(s + 27{\cdot}8 - 1548\mathrm{j})} \times \frac{(s + 26{\cdot}8 + 1560\mathrm{j})(s + 23{\cdot}2 - 42{\cdot}5\mathrm{j})}{(s + 27{\cdot}8 + 1548\mathrm{kj})(s + 251{\cdot}1 - 158{\cdot}6\mathrm{j})} \times \frac{(s + 23{\cdot}2 + 42{\cdot}5\mathrm{j})(s + 600)}{(s + 251{\cdot}1 + 158{\cdot}6\mathrm{j})(s + 40)}. \tag{13}$$

Figure 6 shows the gain plot of the sensitivity function (the transfer function of M from w to z in Figure 3) with weight function in the output path, which represents a nominal performance of the closed-loop control system. In this figure, (a) gives the result of H_∞ control and (b) that of the μ-synthesis. It is found that the nominal performance was improved remarkably when the μ-synthesis was used. The peak value is about 1·9 in Figure 6(a) and 0·92 in (b).

Figure 7 shows the robust performance of the closed-loop system. It is difficult to satisfy the desired performance only if H_∞ is used. However, the robust performance could be satisfied with the peak value less than 1 when the μ-synthesis was used.

4. EXPERIMENTAL SET-UP

The experimental set-up used in this study is shown schematically in Figure 8. The experiment was carried out in a low-speed wind tunnel at the Institute of Fluid Science, Tohoku University. The length of experimental area of the wind tunnel is 0·508 m when the wind tunnel is used in open mode. The nozzle of the wind tunnel is of right octagon cross-section, in which the distance between the opposite sides is 0·297 m at the exit. When the wind tunnel is used in open mode, the velocity of flow can be increased to the maximum value of 65 m/s in the experimental area. The deflection of velocity distribution is less than 0·6% at the velocity of 34 and 60 m/s, and the magnitude of velocity turbulence is less than 0·1%. The mounting table was made of an aluminum plate with the length of 500 mm, the width of 400 mm and the thickness of 30 mm, and was placed at the distance of 100 mm below the center of the nozzle. The elastic beam was made of aluminum with a rectangular cross-section and was fixed vertically to a base plate supported by piezoelectric actuators. The rigid cylinder is mounted at the upper end of the elastic beam and exposed to the air-flow.

A laser sensor was used to measure the displacements at the mid-point of the cylinder. The piezoelectric actuator was driven by a power amplifier. The control input was calculated in a personal computer and amplified by a power amplifier before being applied to the actuators. The experimental results were recorded and analysed using an FFT analyser.

5. RESULTS AND DISCUSSION

The amplitude of vortex-induced vibration varies with the speed of main flow and reaches its peak of about 1 mm at $U_0 = 2{\cdot}4$ m/s. Hence, simulations and experiments were performed at this flow speed. The frequency of vibration equals the natural frequency of the first mode. In the simulation the value chosen for the amplitude of $C_w(t)$ is such that the amplitude of vibration has the same value as in experiment.

Figure 9 shows the simulation results of μ-synthesis control. Figure 9 (a) is the time response of displacement at the mid-point of the cylinder and (b) is the control input. The controller was discretized at a sampling interval of $\Delta T = 1{\cdot}0$ ms. The vortex-induced vibration of the cylinder was effectively suppressed by using output feedback of the designed controller. It is shown that the amplitude of vibration was reduced to less than 1/10 in about 0·3 s after control was started.

Figure 10 gives the experiment results. The amplitude of vibration of the cylinder was reduced almost to zero in a few cycles after the control input was applied to the actuators. It can also be found that the experimental results are in good agreement with the simulation results.

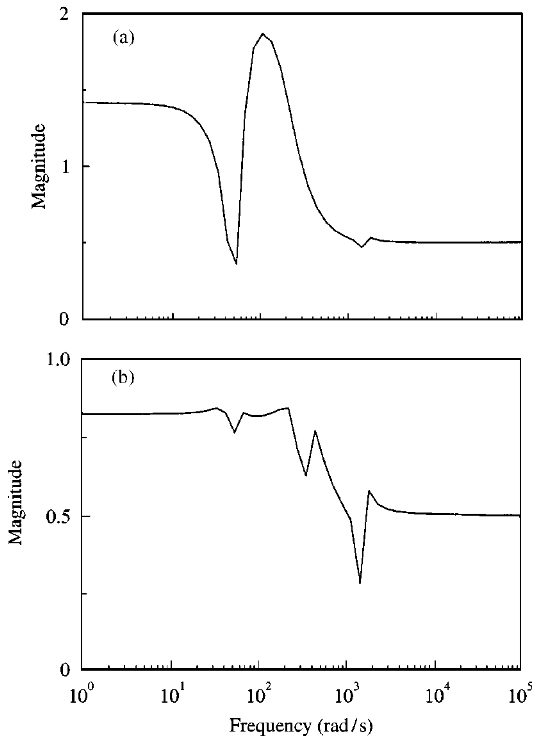

Figure 6. Nominal performance: (a) H_∞ control; (b) μ-synthesis.

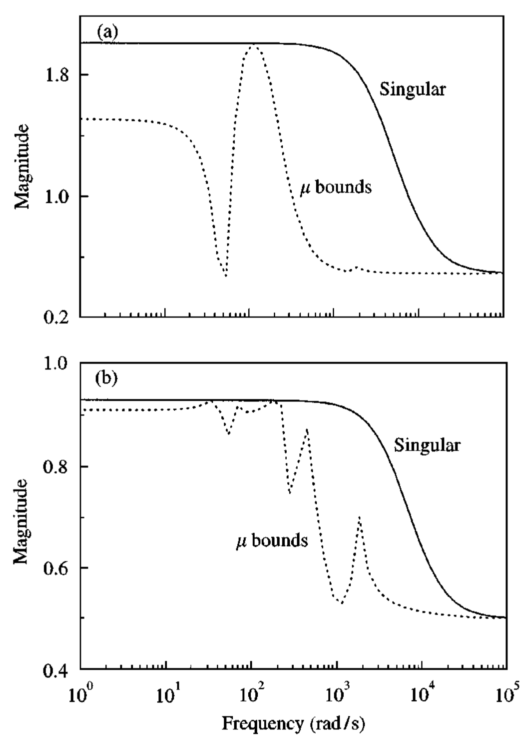

Figure 7. Robust performance: (a) H_∞ control; (b) μ-synthesis.

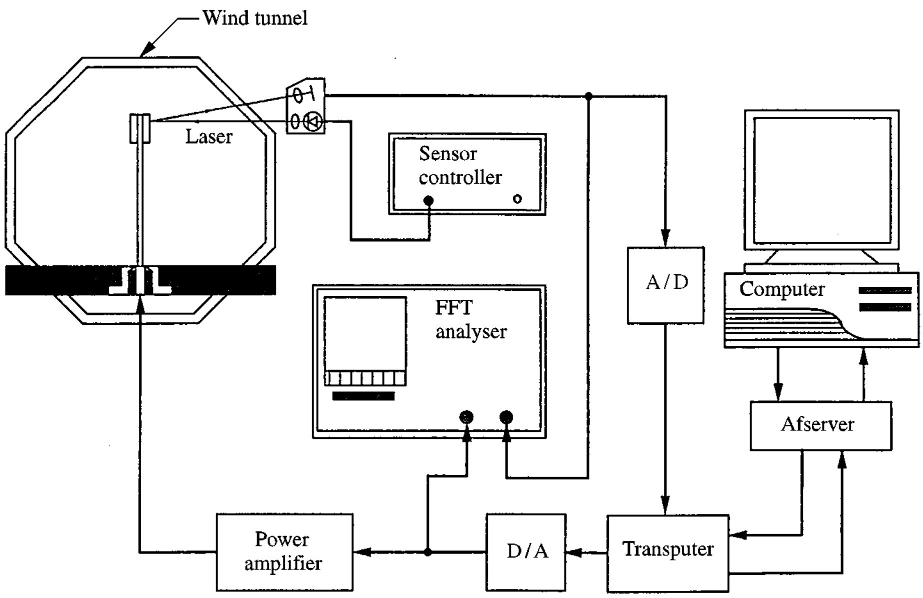

Figure 8. Diagram of experimental set-up.

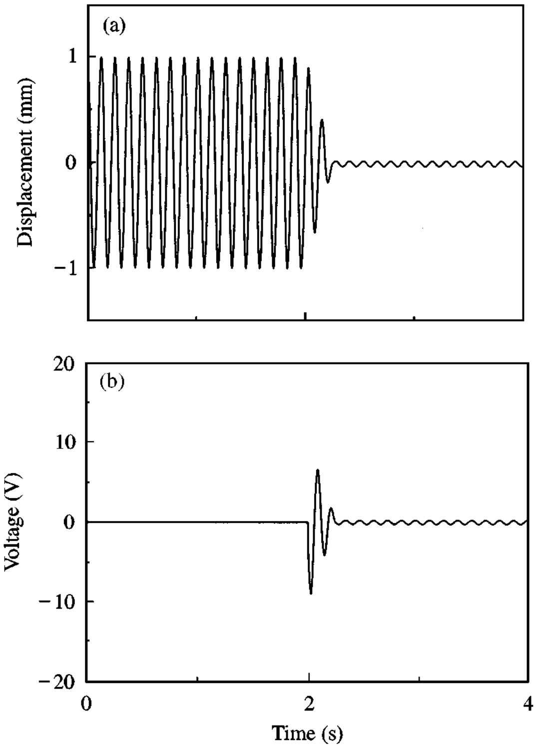

Figure 9. Control effect in simulation: (a) time history of displacement at cylinder mid-point; (b) time history of control input.

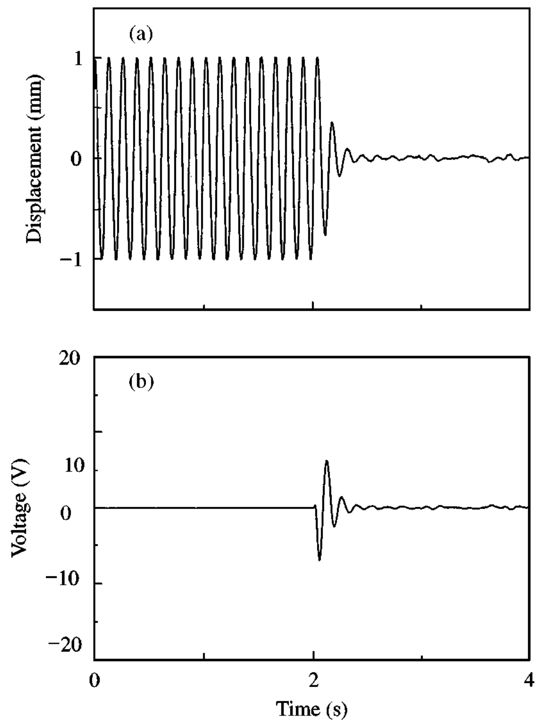

Figure 10. Control effect in experiment: (a) time history of displacement at cylinder mid-point; (b) time history of control input.

6. CONCLUSIONS

Robust control of vortex-induced vibration of a rigid cylinder supported by an elastic beam is investigated numerically and experimentally using μ-synthesis control theory and piezoelectric actuators. From the simulation and experimental results, the following conclusions can be drawn.

1. The robust performance can be greatly improved by applying the μ-synthesis in comparison with the H_∞ control.
2. The vortex-induced vibration of the elastically supported cylinder can be effectively suppressed using μ-synthesis control theory and piezoelectric actuators.

References

Balas, G., Doyle, J., Glover, K., Packard, A. & Smith, R. 1993 *μ Analysis and Synthesis Toolbook User's Guide*. Natick, Massachusetts, U.S.A.: MUSYN Inc.

Baz, A. & Ro, J. 1991 Active control of flow-induced vibrations of a flexible cylinder using direct velocity feedback. *Journal of Sound and Vibration* **146,** 33–45.

Baz, A. & Kim, A. 1993 Active modal control of vortex-induced vibrations of a flexible cylinder. *Journal of Sound and Vibration* **165,** 69–84.

Glover, K. 1984 All optimal Hankel norm approximation of linear multivariable system, and their L_∞-error bounds. *International Journal of Control* **39,** 1145–1193.

Indranil, D. R. & Walter, E. 1996 Adaptive flutter suppression of an unswept wing. *Journal of Aircraft* **33,** 775–783.

Jonathan, D. 1998 Active suppression of aircraft panel vibration with piezoceramic strain actuators. *Journal of Aircraft* **35,** 139–143.

Sumer, B. M. & Fredsoe, J. 1997 *Hydrodynamics around Cylindrical Structures*. Singapore: World Scientific Publishing Co.

APPENDIX: NOMENCLATURE

A	cross-sectional area of the beam
B	cross-sectional size of the elastic beam in the flow direction
C_w	coefficient of lift force
c	internal damping coefficient of the beam
D_s	diameter of the cylinder
d	difference of displacements of the piezoelectric actuators
E	Young's modules
e	perturbation output
G_{nom}	nominal plant
H	cross-sectional size of the elastic beam in the transverse direction
I	area moment of inertia
K	controller
L_b	effective length ($L_b = L - L_s/2$)
L	total length of the beam
L_s	length of the cylinder
l_p	distance between the two actuators
m	mass of the cylinder
$q_j(t)$	modal coordinate
U_0	velocity of air-flow
$u(t)$	control input
$W(x, t)$	deflection of the beam
W_{del}, W_p	weight functions
w	disturbance input
x	coordinate in the longitudinal direction of the beam
y	coordinate in the transverse direction of the beam
$y_c(t)$	output variable
z	error output
$\delta(x)$	dirac delta function
θ	rotation angle of the base plate
v	perturbation input
ρ	density of the elastic beam
ρ_s	air density
$\phi_j(x)$	modal function of the beam
ω_j	angular frequency of jth mode
$\mathbf{A}$, $\mathbf{B}$, $\mathbf{C}$, $\mathbf{F}$	matrices of state equation
$\mathbf{X}(t)$	state vector
$\lVert \cdot \rVert_\infty$	H_∞ norm of a variable